RSC Advances

ROYAL SOCIETY OF CHEMISTRY

www.rsc.org/advances

High-temperature Creep Properties of TATB-based Polymer Bonded Explosives Filled with Multi-walled Carbon Nanotubes

Lin Cong-mei, LIU Jia-hui, Gong Fei-yan, Zeng Gui-yu, Huang Zhong, Pan Li-Ping, Zhang Jian-hu, Liu Shi-jun*

(Institute of Chemical Materials, CAEP, Mianyang 621900, China)

Abstract: In order to investigate the effects of multi-walled carbon nanotubes (MWCNTs) content and loading stress on the high-temperature creep properties of 1,3,5-triamino-2,4,6-trinitrobenzene (TATB)-based polymer bonded explosives (PBXs), three-point bending creep behavior was studied by dynamic mechanical analyzer at 60 ℃. The experimental results showed that under low stress (4 MPa), the constant creep strain rates of the multi-walled carbon nanotubes (MWCNTs) modified formulation reduced with MWCNTs concentration. However, due to the agglomeration of MWCNTs, the existence of intertube sliding or stick-slip resulted in an increase in creep strain. Under higher stress (6 MPa and 7 MPa), with only 0.25 mass% of MWCNTs, the creep resistance of TATB-based PBX could be significantly improved with reduced constant creep strain rate. Additionally, compared with TATB-based PBX without MWCNTs, the creep lifetime of the nanocomposites with content of 0.25 mass% MWCNTs had been considerably extended by over 33.3% and 750% under 6 MPa and 7 MPa, respectively. The nanocomposites with content of 0.5 mass% MWCNTs displayed a lower creep resistance compared to that of TATB-based PBX without MWCNTs. The creep resistance of TATB-based PBXs depends significantly on loading stress. Six-element model could be used to simulate the high-temperature creep behaviors of TATB-based PBXs with and without MWCNTs. The constitutive equations of creep curves under different stresses at 60 ℃ were obtained. Among the fitting parameters, elastic modulus of high elastic deformation E_3 and the viscosity of Voigt units η_3 were sensitive and promising for the evaluation of the creep strain of TATB-based PBXs.

Key words: applied chemistry; TATB; polymer bonded explosive; carbon nanotube; creep properties; constitutive equation

1 Introduction

As a time-dependent mechanism of plastic deformation, creep is the most basic representation of static viscoelastic and one of the main failure forms of polymer material[1-3]. At a certain temperature and loading stress, the creep deformation of polymer has a strong influence on the dimensional stability, long-term durability and reliability. Therefore, improving the creep resistance is a long-term target for polymer[4]. It is found that with the addition of very low content of inorganic nanoparticles, such as clay[5-8], carbon nanotubes(CNTs)[9-13], acicular titania nanoparticles[14], silica nanoparticles[15], the creep resistance of polymer could be significantly improved. However, it is also reported that the addition of nanoparticles, such as clay, reduced the creep resistance of polymer due to the decrease of crystal size and degree of crystallinity[16, 17]. Among the inorganic nanoparticles, as a kind of new quasi-one-dimensional functional material,

* Corresponding Author：Liu Shi-jun, Associate Professor, Institute of Chemical Materials, CAEP, Tel: 86-816-2489302, FAX: 86-816-2495856, email: lsj99@sohu.com

CNTs have attracted intensive interest for a variety of applications in science and engineering during the past decade[18-22], due to the excellent mechanical and physical properties, such as extremely high strength and stiffness, high thermal and electrical conductivity, low density. Up to now, most efforts have been devoted to study the neat polymer/CNTs nanocomposites, such as PP/CNTs composites, polymethylmethacrylate (PMMA) /CNTs composites, epoxy/CNTs composites[9-13]. Yang et al.[9] have found that with only 1 vol.% of multiwalled carbon nanotubes (MWCNTs), creep resistance of polypropylene (PP) can be significantly improved with reduced creep deformation and creep rate at a long-term loading period without sacrificing mechanical properties and weight penalty. Ganß et al. [11] have discussed the result that the nanocomposites exhibited a decrease in creep compliance with the addition of CNTs in the light of polymer/nanotube interaction. It is also revealed that MWCNTs have a more significant effect on the creep resistance of PMMA nanocomposites than that of carbon nanofibers[12].

Due to the moderately energy output and excellent thermally stability, tri-amino-tri-nitro-benzene (TATB) has been comprehensively applied in military field as insensitive high explosive (IHE)[23-27]. TATB-based polymer bonded explosive (PBX) is a kind of particle highly-filled polymer composite. The structure and properties of TATB-based PBX, such as pore structure and size distribution[28,29], microstructural differences between virgin and recycled lots[30], mechanical behavior[31-33], shock initiation[34,35], thermal expansion[36,37], sensitivity[38], moisture outgassing[39], have been widely studied in the past years. However, there are only few literatures concerning creep performance of TATB-based PBX. Gagliardi et al.[40] have carried out high fidelity measurements of time-dependent creep strain in the plastic-bonded explosives LX-17-1 and PBX-9502 and pointed out that the creep and recovery behavior of PBX was dependent on the type of explosive, the percentage and type of binder, the stress level and test temperature.

Less attention is paid to the effects of nanoparticles on the creep resistance of TATB-based PBX. In present study, the creep behaviors of TATB-based PBX prepared with water suspension methods, have been studied by three-point bending creep experiments. An attempt has been made to correlate the observed creep properties of TATB-based PBX with MWCNTs concentration and loading stress.

2 Experimental Section

2.1 Materials

1,3,5-triamino-2,4,6-trinitrobenzene (TATB) (purity 99%, particle size about 14 μm, specific surface area 0.87 m^2/g) was provided by Institute of Chemical Materials, CAEP, China. Fluoropolymer with a weight average molecular weight of 2.74×10^5 g/mol and a polydispersity index of 3.37 was supplied by Zhonghao Chenguang Chemical Industry Co., Ltd. China. Multi-walled carbon nanotubes (MWCNTs) with a length of 5~15 μm and outer diameter of 10~30 nm were obtained from Shenzhen Nanotech Port Co., Ltd. China. The other chemicals and reagents used in this research were commercially purchased and used without further purification.

2.2 Sample Preparation

Three TATB-based formulations including 5 mass% polymer binder were investigated. The original formulation, which contains only TATB and fluoropolymer, is labeled as PBX-1. The modified formulation was prepared with the addition of 0.25 mass% and 0.5 mass% MWCNTs as

reinforcing agent, labeled as PBX-2 and PBX-3, respectively. The molding powders of TATB-based polymer bonded explosives (PBXs) were prepared with water suspension methods[24]. Firstly, TATB (100 g) was added to H_2O (90 mL) and dispersed whilst stirring. Then a fluoropolymer solution with ethyl acetate and butyl acetate (50:50) as solvent was added dropwise, and the system was heated to 70 ℃ in a vacuum. After removing the organic solvent, the precipitate was filtered, washed, and dried in air to give the molding powder of TATB-based PBXs. Afterwards, the molding powder product was pressed in a mould at 120 ℃ under 380 MPa and transformed into explosive sheet with a length of 30 mm, a breadth of 10 mm and a height of 1~2 mm. The pellet density is about 95% of the theoretical density after compression. Morphological characterization was carried out with a field emission scanning electron microscope (FESEM, CamScan Apollo 300, England). The samples were coated with a thin layer of gold in a vacuum chamber for conductivity. The accelerating voltage was 2.0 kV.

2.3 Three-point Bending Creep Test

A creep test can evaluate the creep compliance of material under the constant stress condition. A dynamic mechanical analyzer (DMA 242C, Netzsch, Germany) with a Netzsch three-point bending sample holder was employed to characterize the three-point bending creep properties of the samples. The sample holder with a span of 20 mm was located in a temperature chamber regulated by electrical heating elements in the wall of the chamber, and was brought to the set temperature via heat conduction of the air in the chamber. A small thermocouple was located in the vicinity of the sample to measure the air temperature. The test time was set as 90 min. If no rupture of sample was observed after 90 min, the test stopped. If the creep failure of sample was occurred in the examined time, the test finished immediately.

The schematic of the three-point bending creep experiment was presented in Figure l. The sample was coinstantaneously affected by tensile load and compressive load. The upper surface sufferred from compressive load and the lower surface sufferred from tensile load. At a certain center layer, i.e. neutral layer, no tensile stress or compressive stress was loaded on the sample. The bending normal stress presented a linear distribution perpendicular to the neutral layer. The bending normal stress reached maximum on the surface. The maximum bending normal stress σ_{max} was calculated using the following equation:

$$\sigma_{max} = \frac{3FL}{2wh^2} \quad (1)$$

where F represented the load force, L described the span of sample holder (20 mm), w and h were the sample width and height, respectively.

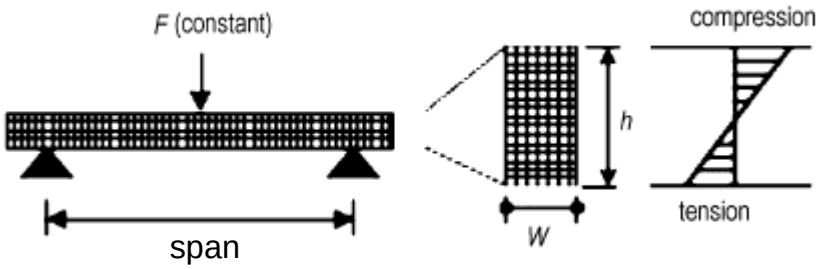

Figure 1. Schematic of three-point bending creep experiment.

3 Results and Discussion

3.1 Morphology of TATB-based PBXs modified with MWCNTs

Figure 2 gives the SEM micrographs of the MWCNTs modified composites PBX-2 and PBX-3 with 0.25 mass% and 0.5 mass% MWCNTs. As shown in Figure 2, the nanotubes are fairly well dispersed in the nanocomposites PBX-2 with lower content of MWCNTs (0.25 mass%). When the filler content increases to 0.5 mass%, it is difficult to completely disperse the MWCNTs in the TATB-based PBX with some small nanotube aggregates.

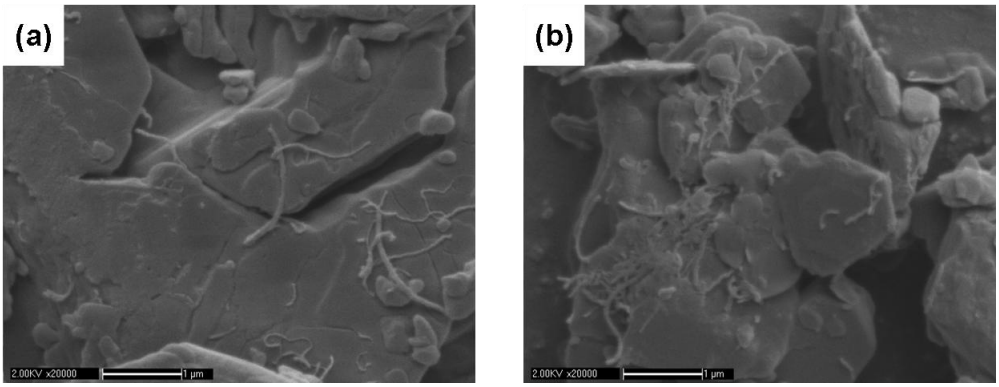

Figure 2. SEM micrographs of MWCNTs modified composites with filler content of (a) 0.25 mass%; (b) 0.5 mass%.

3.2 Three-point Bending Creep Behaviors of TATB-based PBXs

The three-point bending creep strain curves of three TATB-based PBXs at 60 ℃ under different maximum bending normal stresses are shown in Figure 3. Table 1 summarizes the creep performance parameters of TATB-based PBXs. In terms of the creep time, the creep process could be divided into there characteristic stages. In the primary stage, namely, decelerated creep stage, the creep strain rate, i.e. $\triangle\varepsilon/\triangle t$, is found to diminish with increasing creep time. In the secondary stage, namely, steady creep stage, the creep strain rate keeps constant. In the last stage, namely, accelerated creep stage, the creep strain rate increases with creep time. Taken the creep curve of PBX-2 at 60 ℃/7MPa as an example, all these three characteristic stages are marked in Figure 3.

As can be seen in Figure 3 and Table 1, in the experimental set time, no creep rupture is found in the three-point bending creep process of TATB-based PBXs at 60 ℃/4 MPa. Due to the low loading stress, the sample displays a long-term creep process and no creep rupture time could be obtained. Only decelerated creep stage and steady creep stage could be observed from the creep strain curves. The relationship of the creep time on the creep strain in the steady creep stage of PBX-1 at 60 ℃/4 MPa is plotted in Figure 4. It is obvious that the creep strain varies linearly with the creep time in the steady creep stage. The constant creep strain rate is the coefficient of creep strain to creep time which are acquired from the slope of the fitting lines in Figure 4. At 60 ℃/4 MPa, the constant creep strain rate of PBX-1 is 7.51×10^{-5}% min^{-1}. The constant creep strain rates of TATB-based PBXs are listed in Table 1. As revealed shown in Table 2, at 60 ℃/4 MPa, the constant creep strain rates of the multi-walled carbon nanotubes (MWCNTs) modified formulations PBX-2 and PBX-3 are lower than that of the PBX-1. This result could be also explained by the fact that the motion of chain segment of fluoropolymer is restricted by the

presence of MWCNTs. However, an increase of the three-point bending creep strain of MWCNTs modified formulations is observed with increasing MWCNTs content. In fact, due to the fact that MWCNTs are not ideally dispersed in polymer matrix, poor load transfer between nanotubes (in some bundles or entanglements) and between nanotubes and surrounding polymer chains may give rise to interfacial slippage and an increase in the creep strain under low stress[41,42].

Under higher stress (6 MPa and 7 MPa) at 60 ℃, as represented in Figure 3(b) and Figure 3(c), compared with PBX-1 without MWCNTs, with only 0.25 mass% of the reinforcing agent MWCNTs, the creep resistance of PBX-2 is improved with reduced constant creep strain rate and prolonged creep rupture time. For example, at 60 ℃/7 MPa, with regard to PBX-1 without MWCNTs, the creep strain increases rapidly with creep time, afterwards, creep failure of the sample is occurred at 5.0 min with a constant creep strain rate of 4.38×10^{-3}% min^{-1}. The creep rupture time of nanocomposite PBX-2 is considerably extended by 750% compared with that of PBX-1, and the constant creep strain rate distinctly reduces by 86.6%. As a kind of particle highly-filled composite, when the particle phase is rigid, although the polymer content is low, the creep of polymer matrix still is the main source of the creep of composite. Consequently, the creep behavior of TATB-based PBXs depends on the creep properties of polymer binder. Three possible mechanisms of load transfer that could contribute to the observed enhancement of creep resistance are proposed by Yang et al.[9], which are (i) fairly good interfacial strength between MWCNTs and polymer matrix, (ii) increasing immobility of amorphous region due to the appearance of nanotubes acting as blocking sites, and (iii) high aspect ratio of MWCNTs. For MWCNTs/fluoropolymer nanocomposites, the large deformation of fluoropolymer transfers the external load to MWCNTs through the good interfacial bonding. Under the external load, the crack initiates and propagates in the fluoropolymer matrix far from MWCNTs due to the low bulk strength. When propagated to MWCNTs with skin-core structure, the crack branches and deflects, inducing an increase of crack propagation resistance. Furthermore, MWCNTs are randomly distributed in the fluoropolymer matrix and lapped with each other. On account of the high aspect ratio of MWCNTs, skeleton structure is formed to bolck the motion of surrounding molecular chain. Accordingly, a prominent increase of the creep resistance of MWCNTs/fluoropolymer nanocomposites is achieved, resulting in the enhancement of the creep resistance of TATB-based PBXs.

In addition, it should be noted that with 0.5 mass% of MWCNTs, the creep resistance of PBX-3 reduces with increased constant creep strain rate and shortened creep rupture time, compared with PBX-1 without MWCNTs. For example, at 60 ℃/6 MPa, the creep failure of PBX-1 without MWCNTs is occurred at 67.5 min, while the creep failure time of PBX-3 is shortened to 35.5 min. Shen et al.[16] and Beake et al.[17] have studied the nanoindentation behavior of nylon 66/clay nanocomposites and poly(ethylene oxide)/clay nanocomposites, respectively, and also revealed that the addition of small amount of clay had an adverse effect on the creep behavior of the nanocomposites, in accordance with the results of PBX-3 with 0.5 mass% of MWCNTs. Generally, as a result of the addition of nanoparticles, such as clay and carbon nanotubes into the polymer matrix, two adverse effects are functioning simultaneously on the nanocomposites[16]: (i) significant enhancement effect from the well-dispersed, stiff, high aspect ratio nanoparticles, usually and particularly having remarkable influence on hardness and modulus of the material, as observed in PBX-2 with 0.25 mass% of MWCNTs; (ii) substantial changes of micro and/or nano-structures of the matrix due to confinement or other effects, for instance, the changes of

crystalline morphology for semicrystalline thermoplastics owing to heterogeneous nucleation of nanoparticles, which usually lower or destroy the crystal perfection or crystallinity of the polymer matrix, as observed in PBX-3 with 0.5 mass% of MWCNTs. Two competing or combined effects coexist in the TATB-based PBXs. For PBX-3, MWCNTs trends to agglomerate in the polymer matrix. On the other hand, MWCNTs act as heterogeneous nucleating agent in fluoropolymer and thus possibly reduce the crystal size or the degree of crystallinity. The morphological change plays a dominant role in the creep behavior, giving rise to the poor creep resistance of PBX-3.

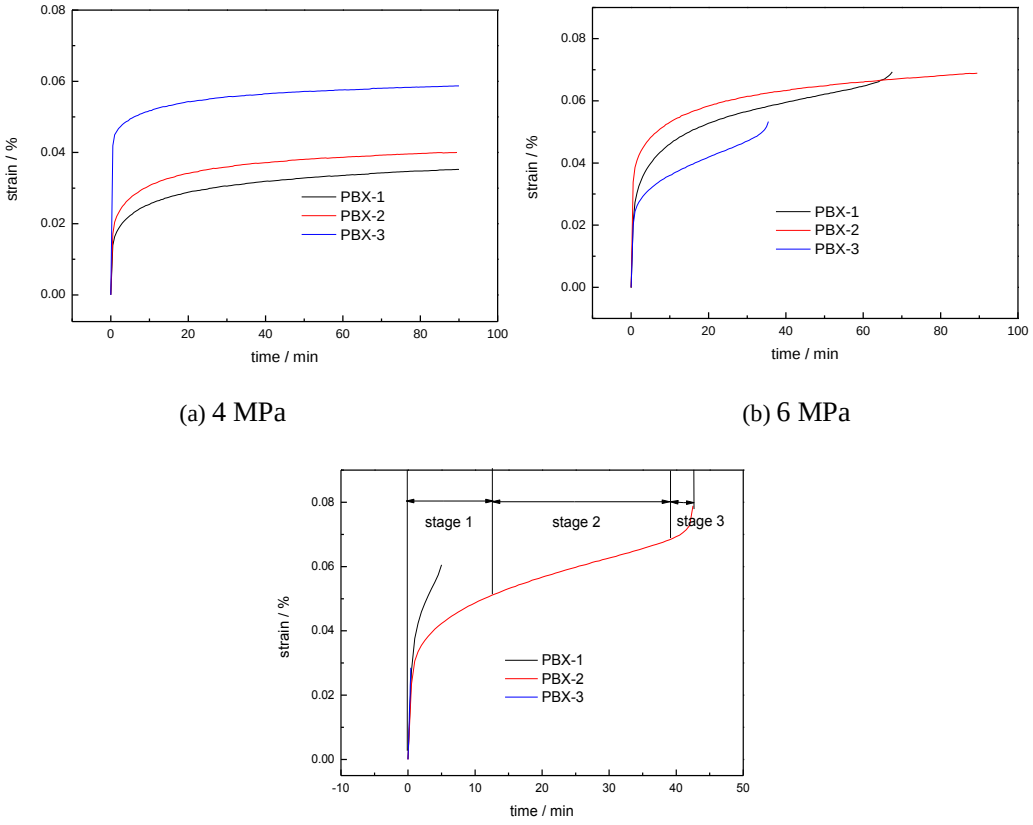

(a) 4 MPa (b) 6 MPa

(c) 7 MPa

Figure 3. Three-point bending creep strain curves of TATB-based PBXs at 60 ℃ under different maximum bending normal stresses.

Table 1. The creep performance parameters of TATB-based PBXs.

sample	maximum bending normal stress / MPa	constant creep strain rate / %.min^{-1}	creep failure strain / %	creep failure time / min
PBX-1	4	7.51×10^{-5}	> 0.03526	> 90
	6	2.65×10^{-4}	0.06931	67.5
	7	4.38×10^{-3}	0.06052	5.0
PBX-2	4	6.43×10^{-5}	> 0.04002	> 90
	6	1.21×10^{-4}	> 0.06887	> 90
	7	5.89×10^{-4}	0.07889	42.5
PBX-3	4	4.96×10^{-5}	> 0.05872	> 90
	6	5.33×10^{-4}	0.05332	35.5
	7	--	0.02854	0.4

Creep is a typical viscoelastic phenomenon of PBX, which is intimately correlated to loading stress. As depicted in Figure 3 and Table 1, the creep resistance depends significantly on the maximum bending normal stress σ_{max}. It is clear that with σ_{max} increased from 4 MPa to 7 MPa at 60 ℃, the creep rupture time of PBX-1 minishes from more than 90 min to 5 min, the creep strain and constant creep strain rate enlarges, suggesting that the creep resistance decreases obviously. The creep resistance of PBX-2 and PBX-3 presents a similar trend with loading stress. The results indicate that the dimensional stability and long-term load capacity reduces with increasing loading stress. The result is attributed to an enhancement in molecular thermodynamic movement. According to free volume theory[43], the viscosity which reflects time-dependence of material is correlated with free volume fraction. An increase in intermolecular free volume fraction is caused by the increase of stress, resulting in a decrease of material viscosity and the aggravation of molecular thermodynamic movement. Consequently, the creep resistance of TATB-based PBXs reduced with increasing stress.

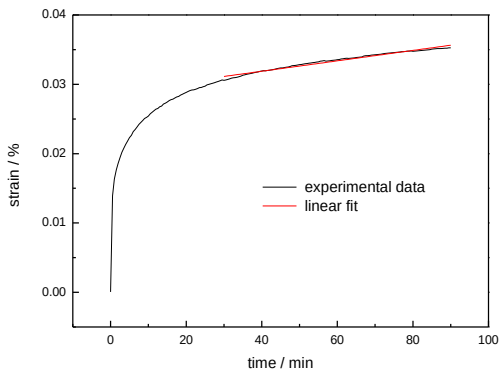

Figure 4. The linear fit of the creep strain curves during steady state of PBX-1 at 60 ℃/4 MPa.

3.2 Constitutive Equation of Creep Curve

In an attempt to deeply understand the creep mechanical relaxation behavior, many researchers propose that the creep process could be simulated by the combination of ideal spring and ideal dashpot in different forms, such as Maxwell model, Voigt (or Kelvin) model and Burger four-element mechanical model[44]。Among them, as a combination of Maxwell and Voigt elements, Burger four-element mechanical model is one of the most used models to give the relationship between the morphology of the composites and their creep behavior[10]. But Burger model only gives the exponential respondence with single relaxation time. PBX is a kind of particle highly-filled composite material based on polymer. On account of the multiplicity of structure units and complexity of molecular motion, not only one relaxation time exist in the creep process. Therefore, multiple element mechanical model should be adopted to simulate the creep process. In this work, a six-element mechanical model is employed to describe the creep process, as shown in Figure 5.

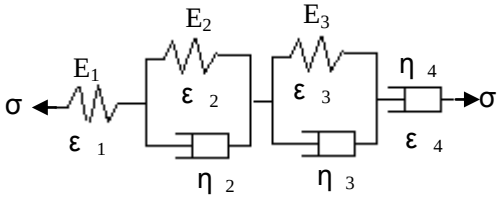

Figure 5. Schematic drawing of six-element mechanical model.

The six-element mechanical model can be regarded as a series connection structure of a Maxwell model and two Voigt models. During the creep process, $\sigma=\sigma_0$, consequently, the total strain of polymer composite material PBX could be determined by:

$$\varepsilon(t)=\varepsilon_1+\varepsilon_2+\varepsilon_3+\varepsilon_4=\frac{\sigma_0}{E_1}+\frac{\sigma_0}{E_2}\left(1-e^{-t/\tau_2}\right)+\frac{\sigma_0}{E_3}\left(1-e^{-t/\tau_3}\right)+\frac{\sigma_0}{\eta_4}t \qquad (2)$$

where ε(t) denotes a function of creep strain ε with creep time t, ε_1 is the instantaneous elastic deformation, ε_2 and ε_3 are the high elastic deformation, ε_4 is the viscous flow deformation, σ_0 is the initial stress, E_1 is the elastic modulus of instantaneous elastic deformation, E_2 and E_3 are elastic modulus of high elastic deformation, τ_2 and τ_3 are the relaxation time, η_4 is the bulk viscosity, respectively. Among them, $\tau_2=\eta_2/E_2$ and $\tau_3=\eta_3/E_3$ represent the time taken to produce 63.2% or $(1-e^{-1})$ of the total deformation in Voigt units, where η_2 and η_3 are related to the viscosity of Voigt units.

Equation 2 divides by σ_0:

$$\frac{\varepsilon(t)}{\sigma_0}=\frac{1}{E_1}+\frac{1}{E_2}\left(1-e^{-t/\tau_2}\right)+\frac{1}{E_3}\left(1-e^{-t/\tau_3}\right)+\frac{1}{\eta_4}t \qquad (3)$$

During the creep process, the loading stress is regarded as a constant value, and therefore, the creep process can be also characterized with the creep compliance D. The creep compliance can be calculated as:

$$D(t)=\frac{\varepsilon(t)}{\sigma} \qquad (4)$$

Equation 3 is transferred to creep compliance equation:

$$D(t)=\frac{1}{E_1}+\frac{1}{E_2}\left(1-e^{-t/\tau_2}\right)+\frac{1}{E_3}\left(1-e^{-t/\tau_3}\right)+\frac{1}{\eta_4}t \qquad (5)$$

Equation 5 is the constitutive equation of creep compliance curve.

As an example, Figure 6 gives the model prediction of the experimental data with the method of non-linear fitting for PBX-1 at 60 ℃/4 MPa using Origin data analysis software. As can be seen in Figure 6, the experimental data can well fit into the six-element mechanical model. The non-linear fitting parameters of six-element model, including the elastic modulus E_1, E_2, E_3, the relaxation time τ_2, τ_3, the viscosity of Voigt units η_2, η_3, and the bulk viscosity η_4 of TATB-based PBXs are listed in Table 3. Square values of fitting correlation coefficient R^2 are all above 0.99865, suggesting that the six-element mechanical model can effectively describe the three-point bending creep behaviors of TATB-based PBXs with high precision.

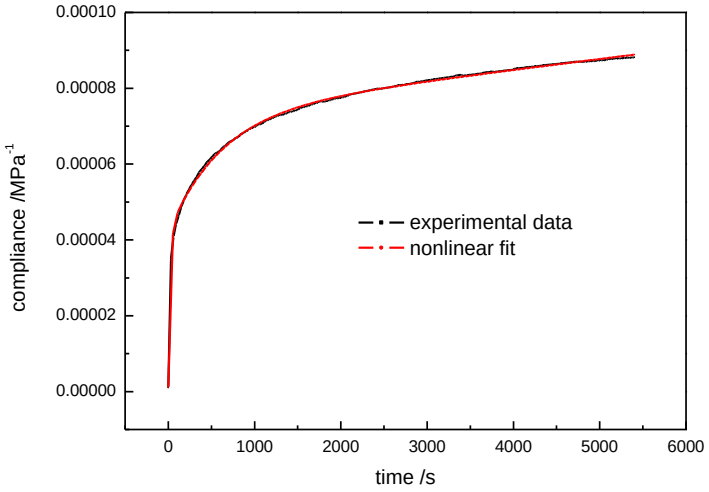

Figure 6. Three-point bending creep compliance curve and non-linear fitting curve of PBX-1 at 60 ℃/4 MPa.

Table 2. The fitting parameters of six-element model under different conditions.

Test condition	sample	E_1 /MPa	E_2 /MPa	τ_2 /s	η_2 /MPa s	E_3 /MPa	τ_3 /s	η_3 /MPa s	η_4 /MPa s	R^2
	PBX-1	8.130×10^5	3.198×10^4	616.17	1.971×10^7	2.445×10^4	21.62	5.286×10^5	3.493×10^8	0.99865
60℃/4MPa	PBX-2	5.291×10^6	2.863×10^4	603.53	1.728×10^7	1.902×10^4	21.48	4.085×10^5	4.106×10^8	0.99869
	PBX-3	5.721×10^7	4.134×10^4	623.76	2.579×10^7	8.856×10^3	12.25	1.085×10^5	5.373×10^8	0.99931
60℃/6MPa	PBX-2	8.464×10^6	3.022×10^4	603.96	1.825×10^7	1.521×10^4	17.90	2.723×10^5	3.270×10^8	0.99894

As can be seen from the fitting parameters in Table 2, the bulk viscosity η_4, which reflects that the irrecoverable creep strain is much higher than the viscosity of Voigt units η_2 and η_3. The bulk viscosity η_4 manifests a distinct depend on MWCNTs content. η_4 increases with increasing MWCNTs concentration, indicating that lower flow was occurred and the permanent deformation reduced. The fact is resulted from the capability of MWCNTs to restrict the relative slide of molecular chain. η_4 is also sensitive to the loading stress. η_4 decreases as the loading stress increases. As mentioned above, the results could be attributed to an increase in intermolecular free volume fraction and an aggravation of molecular thermodynamic movement with increasing loading stress. Among the fitting paremeters, E_3 decreases with MWCNTs concentration under 4 MPa. The results are in good accordance with the change trend of creep strain. The higher value of E_3 implies a smaller creep strain. It is also observed that E_3 decreases with the loading stress, indicating a poor creep resistance. η_3 also displays a similar decrease trend with MWCNTs concentration and loading stress. In view of the results, it seems reasonable to believe E_3 and η_3 could be promising for the evaluation of the creep strain of TATB-based PBXs.

4 Conclusions

Multi-walled carbon nanotubes (MWCNTs) were used as a reinforcing agent in the 1,3,5-triamino-2,4,6-trinitrobenzene (TATB)-based polymer bonded explosives (PBXs) to examine

the influences of MWCNTs and loading stress on the creep properties of TATB-based PBXs. The experimental results demonstrated that:

1. The creep behavior of MWCNTs modified TATB-based PBXs presented a different relationship with the MWCNTs content under low stress and high stress. It was found that under low stress (4 MPa), compared with TATB-based PBX without MWCNTs, the constant creep strain rates of the multi-walled carbon nanotubes (MWCNTs) modified formulations reduced, while creep strain increased. Under higher stress (6 MPa and 7 MPa), with regard to the MWCNTs modified formulation with only 0.25 mass% of MWCNTs, the creep resistance could be significantly improved with reduced constant creep strain rate and prolonged creep lifetime. However, the nanocomposites with content of 0.5 mass% MWCNTs displayed a lower creep resistance compared to that of TATB-based PBX without MWCNTs.
2. Owing to an increase in intermolecular free volume fraction and an aggravation of molecular thermodynamic movement, TATB-based PBXs with or without MWCNTs displayed a very pronounced decrease in the creep resistance with increasing loading stress.
3. Six-element model was utilized to simulate the relaxation process of creep process of TATB-based PBXs. The experimental results indicated that the bulk viscosity η_4 manifests a distinct depend on the content of MWCNTs, due to the capability of MWCNTs to diminish the relative slip of polymer chains. Elastic modulus of high elastic deformation E_3 and the viscosity of Voigt units η_3 were sensitive and promising for the evaluation of the creep strain of TATB-based PBXs.

References

1 Y. Tajima, T. Itoh, Creep rupture properties of homopolymer, copolymer, and terpolymer based on poly(oxymethylene), Journal of Applied Polymer Science, 2010, 116, 3242-3248.

2 P. Berthoud; C. G'. Sell;.J. M. Hiver, Elastic-plastic indentation creep of glassy poly(methyl methacrylate) and polystyrene: characterization using uniaxial compression and indentation tests, Journal of Physics D: Applied Physics, 1999, 32, 2923-2932.

3 A. Habas-Ulloa, J-R. M. D'Almeida, J-P. Habas, Creep behavior of high density polyethylene after aging in contact with different oil derivates, Polymer Engineering and Science, 2010, 50, 2122-2130.

4 T. H. Zhou, W. H. Ruan, J. L. Yang, M. Z. Rong, M. Q. Zhang , Z. Zhang, A novel route for improving creep resistance of polymers using nanoparticles, Composites Science and Technology, 2007, 67, 2297-2302.

5 A. Ranade, K. Nayak, D. Fairbrother, N. A. D'Souza, Maleated and non-maleated polyethylene–montmorillonite layered silicate blown films: creep, dispersion and crystallinity, Polymer, 2005, 46, 7323-7333.

6 A. Pegoretti, J. Kolarik, C. Peroni, C. Migliaresi, Recycled poly(ethylene terephthalate)/layered silicate nanocomposites: morphology and tensile mechanical properties, Polymer, 2004, 45, 2751-2759.

7 S. Siengchin, J. Karger-Kocsis, Creep Behavior of Polystyrene/Fluorohectorite Micro- and Nanocomposites, Macromolecular Rapid Communications, 2006, 27, 2090-2094.

8 H. S. Xia, M. Song, Z. Y. Zhang, M. Richardson, Microphase separation, stress relaxation, and creep behavior of polyurethane nanocomposites, Journal of Applied Polymer Science, 2007,

103, 2992-3002.
9 J. L. Yang, Z. Zhang, K. Friedrich, et al. Creep resistant polymer nanocomposites reinforced with multiwalled carbon nanotubes[J]. Macromolecular Rapid Communications, 2007, 28: 955-961.
10 Y. Jia, K. Peng, X. L. Gong, et al. Creep and recovery of polypropylene/carbon nanotube composites[J]. International Journal of Plasticity, 2011, 27: 1239-1251.
11 M. Ganß, B. K. Satapathy, M. Thunga, et al. Temperature dependence of creep behavior of PP-MWNT nanocomposites[J]. Macromolecular Rapid Communications, 2007, 28: 1624-1633.
12 H. Varela-Rizo, M. Weisenberger, D. R. Bortz, et al. Fracture toughness and creep performance of PMMA composites containing micro and nanosized carbon filaments[J]. Composites Science and Technology, 2010, 70: 1189-1195.
13 M. Tehrani, M. Safdari, M. S. Al-Haik. Nanocharacterization of creep behavior of multiwall carbon nanotubes/epoxy nanocomposite[J]. International Journal of Plasticity, 2011, 27: 887-901.
14 F. Bondioli, A. Dorigato, P. Fabbri, M. Messori, A. Pegoretti, Improving the creep stability of high-density polyethylene with acicular titania nanoparticles, Journal of Applied Polymer Science, 2009, 112, 1045-1055.
15 H. Münstedt, T. Köppl, C. Triebel, Viscous and elastic properties of poly(methyl methacrylate) melts filled with silica nanoparticles, Polymer, 2010, 51, 185-191.
16 L. Shen, I. Y. Phang, L. Chen, et al. Nanoindentation and morphological studies on nylon 66 nanocomposites.I. Effect of clay loading[J]. Polymer, 2004, 45: 3341-3349.
17 B. D. Beake, S. Chen, J. B. Hull , et al. Nanoindentation behavior of clay/poly(ethylene oxide) nanocomposites. J. Nanosci Nanotechnol, 2002, 2, 73-79.
18 S. Iijima. Helical microtubules of graphitic carbon, 1991, 354, 56-58.
19 M. Trujillo, M. L. Arnal, A. J. Müller, E. Laredo, St. Bredeau, D. Bonduel, Ph. Dubois, Thermal and Morphological Characterization of Nanocomposites Prepared by in-Situ Polymerization of High-Density Polyethylene on Carbon Nanotubes. Macromolecules, 2007, 40, 6268-6276.
20 Kangbo Lu; Nadia Grossiord; Cor E. Koning; Hans E. Miltner; Bruno van Mele;Joachim Loos Carbon Nanotube/Isotactic Polypropylene Composites Prepared by Latex Technology: Morphology Analysis of CNT-Induced Nucleation. Macromolecules, 2008, 41, 5753-5762.
21 K. Wang, C. Y. Tang, P. Zhao, H. Yang, Q. Zhang, R. N. Du, Q. Fu, Rheological Investigations in Understanding Shear-Enhanced Crystallization of Isotactic Poly(propylene)/Multi-Walled Carbon Nanotube Composites. Macromolecular Rapid Communications, 2007, 28, 1257-1264.
22 M. Li, Z. Kang, R. Li, X. H. Meng, Y. J. Lu, A molecular dynamics study on tensile strength and failure modes of carbon nanotube junctions, Journal of Physics D: Applied Physics, 2013, 46, 495301.
23 G. C. Yang, F. D. Nie, H. Huang, L. Zhao, W. T. Pang. Preparation and Characterization of Nano-TATB Explosive. Propellants, Explosives, Pyrotechnics, 2006, 31, 390-394.
24 Z. J. Yang, J. S. Li, B. Huang, S. J. Liu, Z. Huang, F. D. Nie. Preparation and Properties Study of Core-Shell CL-20/TATB Composites, Propellants, Explosives, Pyrotechnics, 2014, 39, 51-58.
25 J. T. Mang, R. P. Hjelm, Fractal Networks of Inter-Granular Voids in Pressed TATB.

Propellants, Explosives, Pyrotechnics, 2014, 38, 831-840.
26 R. H. Gee, A. Maiti, L. E. Fried. Mesoscale modeling of irreversible volume growth in powders of anisotropic crystals. Applied Physics Letters, 2007, 90, 254105.
27 S. Roszak, R. H. Gee, K. Balasubramanian, et al. Molecular interactions of TATB clusters[J]. Chemical Physics Letters, 2003, 374: 286-296.
28 T. Darla, B. Geoff, M. Joseph, P. Brian, G. Richard, T. Salyer, D. Racci, Characterizing the Pore Structure and Effects of Ratchet Growth on PBX 9502, 16th APS Topical Conference on Shock Compression of Condensed Matter, June 28-July 3, 2009.
29 T. M. Willey, T. van Buuren, J. R. I. Lee, et al. Changes in pore size distribution upon thermal cycling of TATB-based explosives measured by ultra-small angle X-ray scattering[J]. Propellants, Explosives, Pyrotechnics, 2006, 31(6): 466-471.
30 P. D. Peterson, D. J. Idar, Microstructural Differences between Virgin and Recycled Lots of PBX 9502, Propellants, Explosives, Pyrotechnics, 2005, 30, 88-94.
31 Groves, B. Cunningham, Tensile and Compressive Mechanical Properties of Billet Pressed LX17-1 as a Function of Temperature and Strain Rate. UCRL-ID-137477, 2000.
32 O. Pruneda, R. R. McGuire, R. E. Clements, Development of a High Tensile Strain Pastic Bonded TATB Explosive, UCRL-102395.
33 M. Benziger, et al., X-0298 A Rubber-bonded PBX, LA-8436-MS,1980.
34 R. L. Gustavsen, R. J. Gehr, S. M. Bucholtz, R. R. Alcon, B. D. Bartram, Shock initiation of the tri-amino-tri-nitro-benzene based explosive PBX 9502 cooled to -55° C, Journal of Applied Physics, 2012, 112, 074909.
35 R. L. Gustavsen, S. A. Sheffield, R. R. Alcon, Measurements of shock initiation in the tri-amino-tri-nitro-benzene based explosive PBX 9502: Wave forms from embedded gauges and comparison of four different material lots, Journal of Applied Physics,.2006, 99, 114907.
36 C. Souers, P. Lewis, M. Hoffman, B. Cunningham, Thermal Expansion of LX-17, PBX 9502, and Ultrafine TATB, Propellants, Explosives, Pyrotechnics, 2011, 36, 335-340.
37 H. F. Rizzo, J. R. Humphrey, J. R. Kolb. Growth of 1,3,5-triamino-2,4,6-trinitrobenzene (TATB). Ⅱ.Control of growth by use of high Tg polymeric bingers, UCRL-81189,1980.
38 R. N. Mulford, J. A. Romero, Sensitivity of the TATB-based explosive PBX-9502 after thermal expansion, AIP Conf. Proc. 1998, 429, 723.
39 W. Small IV, E. A. Glascoe, G. E. Overturf. Measurement of moisture outgassing of the plastic-bonded TATB explosive LX-17[J]. Thermochimica Acta, 2012, 545: 90-95.
40 F. J. Gagliardi, B. J. Cunningham. Creep Testing Plastic-Bonded Explosives in Uni-axial Compression, LLNL-CONF-402307, 2008.
41 M. F. Yu, B. I. Yakobson, R. S. Ruoff, Controlled Sliding and Pullout of Nested Shells in Individual Multiwalled Carbon Nanotubes. J. Phys. Chem. B 2000, 104, 8764-8767
42 J. Suhr, N. Koratkar, P. Keblinski, P. Ajayan, Viscoelasticity in carbon nanotube composites, Nature Materials, 2005, 4, 134-137.
43 K. Stefan, Advanced topics in the application of the WLF/free volume theory to high sugar/biopolymer mixtures: a review. Food Hydrocolloids, 2001, 15, 631-641.
44 S. Y. Lee, H. S. Yang, H. J. Kim, C. S. Jeong, B. S. Lim, J. N. Lee, Creep behavior and manufacturing parameters of wood flour filled polypropylene composites. Composite structures, 2004, 65, 459-469.

A table of contents entry

The addition of 0.25 mass% MWCNTs is a simple and novel route for improving creep resistance of TATB-based PBX.